This article was downloaded by: [Institute Of Atmospheric Physics]
On: 09 December 2014, At: 15:20
Publisher: Taylor & Francis
Informa Ltd Registered in England and Wales Registered Number: 1072954 Registered office: Mortimer House, 37-41 Mortimer Street, London W1T 3JH, UK

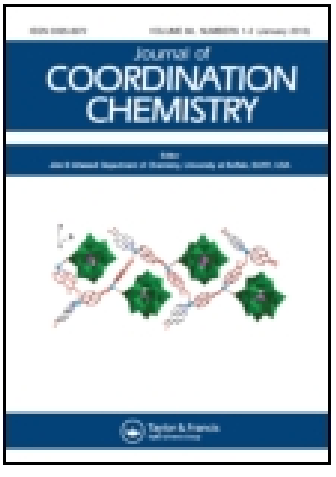

CrossMark
Click for updates

Journal of Coordination Chemistry
Publication details, including instructions for authors and subscription information:
http://www.tandfonline.com/loi/gcoo20

Synthesis, spectral characterization, and anticancer activity of 6-methylpyridine-2-carbaldehdyethiosemicarbazone and its complexes; crystal structure and DFT calculations of [Pd(mpyptsc)Cl]·DMSO

Shadia A. Elsayed[a], Ian S. Butler[b], Denis F.R. Gilson[b], Bertrand J. Jean-Claude[c] & Sahar I. Mostafa[d]

[a] Faculty of Science, Department of Chemistry, Damietta University, New Damietta, Egypt

[b] Department of Chemistry, McGill University, Montreal, Canada

[c] Department of Medicine, Royal Victoria Hospital, Montreal, Canada

[d] Faculty of Science, Department of Chemistry, Mansoura University, Mansoura, Egypt

Accepted author version posted online: 08 Jul 2014.Published online: 08 Aug 2014.

To cite this article: Shadia A. Elsayed, Ian S. Butler, Denis F.R. Gilson, Bertrand J. Jean-Claude & Sahar I. Mostafa (2014) Synthesis, spectral characterization, and anticancer activity of 6-methylpyridine-2-carbaldehdyethiosemicarbazone and its complexes; crystal structure and DFT calculations of [Pd(mpyptsc)Cl]·DMSO, Journal of Coordination Chemistry, 67:16, 2711-2727, DOI: 10.1080/00958972.2014.942224

To link to this article: http://dx.doi.org/10.1080/00958972.2014.942224

PLEASE SCROLL DOWN FOR ARTICLE

Taylor & Francis makes every effort to ensure the accuracy of all the information (the "Content") contained in the publications on our platform. However, Taylor & Francis, our agents, and our licensors make no representations or warranties whatsoever as to the accuracy, completeness, or suitability for any purpose of the Content. Any opinions and views expressed in this publication are the opinions and views of the authors, and are not the views of or endorsed by Taylor & Francis. The accuracy of the Content should not be relied upon and should be independently verified with primary sources

of information. Taylor and Francis shall not be liable for any losses, actions, claims, proceedings, demands, costs, expenses, damages, and other liabilities whatsoever or howsoever caused arising directly or indirectly in connection with, in relation to or arising out of the use of the Content.

This article may be used for research, teaching, and private study purposes. Any substantial or systematic reproduction, redistribution, reselling, loan, sub-licensing, systematic supply, or distribution in any form to anyone is expressly forbidden. Terms & Conditions of access and use can be found at http://www.tandfonline.com/page/terms-and-conditions

Downloaded by [Institute Of Atmospheric Physics] at 15:20 09 December 2014

Journal of Coordination Chemistry, 2014
Vol. 67, No. 16, 2711–2727, http://dx.doi.org/10.1080/00958972.2014.942224

Taylor & Francis
Taylor & Francis Group

Downloaded by [Institute Of Atmospheric Physics] at 15:20 09 December 2014

Synthesis, spectral characterization, and anticancer activity of 6-methylpyridine-2-carbaldehdyethiosemicarbazone and its complexes; crystal structure and DFT calculations of [Pd(mpyptsc)Cl]·DMSO

SHADIA A. ELSAYED†, IAN S. BUTLER*‡, DENIS F.R. GILSON‡, BERTRAND J. JEAN-CLAUDE§ and SAHAR I. MOSTAFA*¶

†Faculty of Science, Department of Chemistry, Damietta University, New Damietta, Egypt
‡Department of Chemistry, McGill University, Montreal, Canada
§Department of Medicine, Royal Victoria Hospital, Montreal, Canada
¶Faculty of Science, Department of Chemistry, Mansoura University, Mansoura, Egypt

(*Received 20 August 2013; accepted 13 June 2014*)

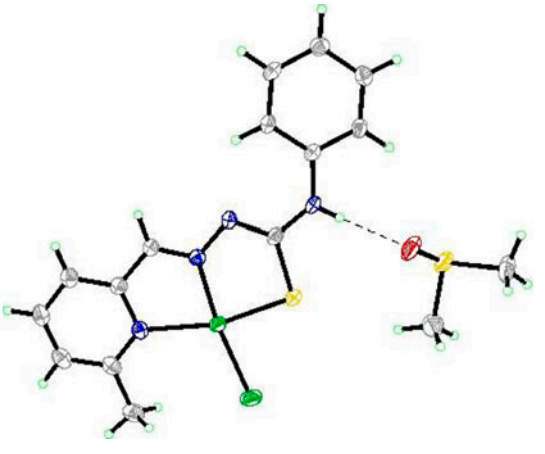

New complexes of 6-methylpyridine-2-carbaldehydethiosemicarbazone (Hmpytsc) and 6-methylpyridine-2-carbaldehyde-N(4)-phenylthiosemicarbazone (Hmpyptsc) and crystal structure of [Pd(mpyptsc)Cl]·DMSO are reported. Hmpyptsc and its complexes were tested against human colon cancer (HCT116) and prostate cancer (DU145) cell lines.

Synthesis and characterization of new complexes of 6-methylpyridine-2-carbaldehydethiosemicarbazone (Hmpytsc) and 6-methylpyridine-2-carbaldehyde-N(4)-phenylthiosemicarbazone (Hmpyptsc) with $[VO_2L]$, $[Zn(HL)Cl_2]$, $[Ru(PPh_3)_2L_2]$, and [MLCl] (M(II) = Pd, Pt; HL = Hmpytsc, Hmpyptsc) are reported. Their structures are discussed on the basis of IR, Raman, UV–vis, NMR (^1H, ^{13}C, and ^{31}P), and mass spectroscopic data, as well as elemental analysis and molar conductivity. In the X-ray crystal structure of the square-planar [Pd(mpyptsc)Cl]·DMSO, mpyptsc$^-$ is coordinated to Pd(II) in a tridentate manner through pyridyl N, azomethine N, and thiol S, and the fourth coordination site is occupied by a

*Corresponding authors. Email: ian.butler@mcgill.ca (I.S. Butler); sihmostafa@gmail.com (S.I. Mostafa)

© 2014 Taylor & Francis

chloride. A theoretical study on [Pd(mpyptsc)Cl]·DMSO was undertaken through DFT conformational analysis. The *in vitro* cytotoxic activity has been evaluated against human colon cancer (HCT116) and prostate cancer (DU145) cell lines. Hmpyptsc and [Zn(Hmpyptsc)Cl_2] were most active with mean IC_{50} values of 3.32 and 2.60 (HCT116), and 3.60 and 3.10 (DU145) μM, respectively.

Keywords: Hmpytsc; Hmpyptsc; Palladium; Zinc; Platinum; Anticancer

Downloaded by [Institute Of Atmospheric Physics] at 15:20 09 December 2014

1. Introduction

The chemistry and biological activity of thiosemicarbazone derivatives and their complexes are of considerable interest [1–6]. In our laboratory, the chemistry of thiosemicarbazones has been an extremely active area of research because of the beneficial biological activities (anticancer, antifungal, and antibacterial) of their transition metal complexes [7–9]. We have reported the chemistry of 2-hydroxybenzophenone-N(4)-(Me, Ph and piperidyl) thiosemicarbazones, 2-formylpyridinethiosemicarbazone, and 6-methylpyridine-2-carbaldehyde-N(4)-ethylthiosemicarbazone, and a number of their transition metal complexes [7–9]. The anticancer activity of 6-methylpyridine-2-carbaldehyde-N(4)-ethylthiosemicarbazone and its Zn(II) and Pd(II) complexes have been tested against colon cancer human cell lines (HCT116) [9]. Over the past few years, our laboratory has been actively involved in the synthesis of O,O-; O,N-; N,S-; N,N,S-; and O,N,S-donor transition metal complexes, which have been evaluated as anticancer agents against *Ehrlich ascites* tumor cells [10–13] and human cancer cell lines [9, 14, 15]. As a part of our continuing interest in the anticancer activity of N,N,S-donor complexes, the present study includes the interaction of 6-methylpyridine-2-carbaldehyde thiosemicarbazone (Hmpytsc) and 6-methylpyridine-2-carbaldehyde-N(4)-phenylthiosemicarbazone (Hmpyptsc) with V(V), Zn(II), Ru(II), Pd(II), and Pt(II). Their structures are discussed on the basis of elemental analysis, molar conductivity, IR, Raman, NMR, and mass spectroscopy. The X-ray crystal structure of [Pd(mpyptsc)Cl]·DMSO is reported. The DFT conformational analysis of [Pd(mpyptsc)Cl]·DMSO was undertaken. The results of the *in vitro* cytotoxic activity of Hmpytsc, Hmpyptsc and their complexes [Zn(HL)Cl_2], and [MLCl] (M(II) = Pd, Pt) have been evaluated against human colon cancer (HCT116) and prostate cancer (DU145) cell lines.

2. Experimental

2.1. *Materials and measurements*

All reagents and solvents were purchased from Alfa-Aesar, and all manipulations were performed under aerobic conditions using materials and solvents as received. The starting complex, [Ru(PPh_3)$_2Cl_2$], was prepared by the literature methods [16]. DMSO-d_6 was used for the NMR measurements, which were referenced against TMS.

The human colon cancer (HCT116) and prostate cancer (DU145) cell lines were obtained from the American Type Culture Collection (ATCC catalog number). Cells were maintained in Roswell Park Memorial Institute (RPMI-1640) medium (Wisent Inc., St-Bruno, Canada) supplemented with 10% fetal bovine serum (FBS), 10 mM HEPES, 2 mM L-gutamine, and 100 μg/mL penicillin/streptomycin (GibcoBRL, Gaithersburg, MD). All assay cells were plated 24 h before drug treatment.

Downloaded by [Institute Of Atmospheric Physics] at 15:20 09 December 2014

Elemental analyses and X-ray crystallography were performed at the Department of Chemistry, Montreal University. The crystal structure was measured at the X-ray Crystal Structure Unit using a Bruker Platform diffractometer equipped with a Bruker MART 4 K Charger-Coupled Device Area Detector using APEX II and a Nonius Fr591 rotating anode (copper radiation) equipped with Montel 200 optics. The crystal-to-detector distance was 5 cm and the data collection was carried out in 512×512 pixel mode. The initial unit-cell parameters were determined by least-squares fit of the angular setting of strong reflections, collected by a 10.0-degree scan in 33 frames over three different parts of the reciprocal space (99 frames total) and one complete sphere of data was collected. Infrared spectra were recorded on a Nicolet 6700 Diamond ATR spectrometer from 4000 to 200 cm^{-1}. Raman spectra were measured on an In-via Renishaw spectrometer using 785-nm laser excitation. NMR spectra were recorded on a VNMRS 500-MHz spectrometer in DMSO-d_6 using TMS as reference. Mass spectra, ESI-MS, and EI-MS were recorded using LCQ Duo and double-focusing MS25RFA instruments, respectively. Electronic spectra were measured in DMF using a Hewlett-Packard 8453 spectrophotometer. Molar conductivity measurements were carried out at room temperature on a YSI Model 32 conductivity bridge. The GAUSSIAN 03 rev B-02 suite of programs was used for the DFT calculations using the DGDZVP/B3LYP basis set [17].

2.2. *Preparations*

Both 6-methylpyridine-2-carbaldehydethiosemicarbazone (Hmpytsc) and 6-methylpyridine-2-carboxaldehyde-N(4)-phenylthiosemicarbazone (Hmpyptsc) were prepared by modification of the literature methods [18].

2.2.1. 6-Methylpyridine-2-carbaldehydethiosemicarbazone (Hmpytsc). 6-Methylpyridine-2-carboxaldehyde (1.21 g, 10 mM) in ethanol (10 mL) was added to thiosemicarbazide (0.91 g, 10 mM) in ethanol-water (1 : 1, V/V; 80 mL) followed by addition of drops of glacial acetic acid. The reaction mixture was heated under reflux for 4 h. The white precipitate was filtered off and washed with water and ethanol. It was re-crystallized from ethanol and dried in *vacuum*. Yield: 89%, m.p. = 219 °C, Elemental Anal. Calcd $C_8H_{10}N_4S$ (%): C, 49.4; H, 5.2; N, 28.8; S, 16.5. Found (%): C, 49.3; H, 5.0; N, 28.6; S, 16.4. IR (Raman) cm^{-1}, 3392, $\nu_{as}(NH_2)$; 3258, $\nu_s(NH_2)$; 3152 ν(NH); 1612 (1808) ν(C=N); 990 (990) ν(N–N); 842, ν(C=S); 623 (630), ρ(Py); ^{1}H NMR (d_6-DMSO/TMS, ppm), δ: 8.056 (d,1H, H_3); 7.66 (t, 1H, H_4); 7.20 (d, 1H, H_5); 8.01 (s, 1H, H_7), 2.43 (s, 3H, CH_3); 11.61 (s, 1H, N(3)H); 8.12, 8.13 (s, 1H, N(4)H_2); ^{13}C NMR (d_6-DMSO/TMS, ppm) δ: 158.3, C(2); 124.1, C(3); 137.4, C(4); 117.9, C(5); 153.5, C(6); 143.5, (CH=N); 178.9, (C=S); 24.5, 6-CH_3.

2.2.2. 6-Methylpyridine-2-carboxaldehyde-N(4)-phenylthiosemicarbazone (Hmpyptsc). The same procedure of preparation of Hmpytsc was applied using N(4)-phenylthiosemicarbazide (1.73 g, 10 mM) instead of thiosemicarbazide. Yield: 85%, m.p. = 184 °C. Elemental Anal. Calcd $C_{14}H_{14}N_4S$ (%): C, 62.2; H, 5.2; N, 20.7; S, 11.8. Found (%): C, 62.0; H, 5.2; N, 20.6; S, 11.7. IR (Raman) cm^{-1}: 3319 (3099), ν(NH); 1588 (1606), ν(C=N); 994 (995), ν(N–N); 784 (792), ν(CS); 643 (597), ρ(Py); ^{1}H NMR (d_6-DMSO/TMS, ppm), δ_H: 8.18 (d, 1H, H_3); 7.72 (t, 1H, H_4); 7.55 (d, 1H, H_5); 8.13 (s, 1H, H7); 2.47 (s, 3H, CH_3); 12.01(s,

1H, N(3)H); 10.30 (s, 1H, N(4)H); 7.20–7.40 (m, ph); ^{13}C NMR (d_6-DMSO/TMS, ppm) δ: 158.2, C(2); 125.8, C(3); 137.1, C(4); 118.5, C(5); 152.5, C(6); 143.6, (CH=N); 176.8 (C=S); 24.2 CH_3; 124.1–138.4, Ph.

2.2.3. [VO_2L] (L = mpytsc, mpyptsc). Solid [$VO(acac)_2$] (0.078 g, 0.3 mM) was added to Hmpytsc or Hmpyptsc (0.3 mM) in ethanol (10 mL). The reaction mixture was stirred and heated under reflux for 1 h. Upon cooling, an orange precipitate was obtained, filtered off, washed with ethanol and diethyl ether and dried in *vacuum*.

2.2.3.1. *For [VO_2(mpytsc)].* Yield: 75%. Elemental Anal. Calcd $C_8H_9N_4O_2SV$ (%): C, 34.7; H, 3.3; N, 20.3; S, 11.6. Found (%): C, 34.7; H, 3.1; N, 20.2; S, 11.5. Conductivity data (10^{-3} M in DMF): $\Lambda_M = 5.0\,\Omega^{-1}$. IR (Raman) cm^{-1}: 3310, $\nu_{as}(NH_2)$; 3277, $\nu_s(NH_2)$; 1632 (1620), ν(C=N); 1020 (1023) ν(N–N); 785, ν(C=S); 634 (681), ρ(Py); 451 (451) ν(V–N); 340 (344), ν(V–S); 936, $\nu_s(VO_2)$; 908, $\nu_{as}(VO_2)$; ^{1}H NMR (d_6-DMSO/TMS, ppm), δ: 7.55 (d, 1H, H_3); 8.10 (t, 1H, H_4); 7.71 (d, 1H, H_5); 8.48 (s, 1H, H_7); 2.48 (s, 3 H, CH_3); 7.87 (s, 2H, N(4)H_2); ^{13}C NMR (d_6-DMSO/TMS, ppm) δ: 158.9, C(2); 123.8, C(3); 137.2, C(4); 117.8, C(5); 154.1, C(6); 144.2, (CH=N); 174.7, (C=S); 24.3, 6-CH_3.

2.2.3.2. *For [VO_2(mpyptsc)].* Yield: 79%. Elemental Anal. Calcd $C_{14}H_{13}N_4O_2SV$ (%): C, 47.7; H, 3.7; N, 15.9; S, 9.1. Found (%): C, 47.3; H, 3.4; N, 15.7; S, 9.0. Conductivity data (10^{-3} M in DMF): $\Lambda_M = 6.0\,\Omega^{-1}$. IR (Raman) cm^{-1}: 3340, ν(NH); 1599 (1613), ν(C=N); 1020 (1022), ν(N–N); 760 (758), ν(C=S); 649 (678), ρ(Py); 446 (449), ν(V–N); 329 (333), ν(V–S); 940, $\nu_s(VO_2)$; 912, $\nu_{as}(VO_2)$; ^{1}H NMR (d_6-DMSO/TMS, ppm), δ: 7.80 (d, 1H, H_3); 8.15 (t, 1H, H_4); 7.70 (d, 1H, H_5); 8.82 (s, 1H, H_7) 2.48 (s, 3H, CH_3); 10.15 (s, 1H, N (4)H); 7.07–7.63 (m, ph); ^{13}C NMR (d_6-DMSO/TMS, ppm) δ: 163.4, C(2); 124.2, C(3); 140.6, C(4); 121.2, C(5); 157.2, C(6); 153.1, (CH=N); 173.6, (C=S); 26.4, CH_3, 123.7–142.8, Ph.

2.2.4. [Zn(HL)Cl_2] (HL = Hmpytsc or Hmpyptsc). Hmpytsc or Hmpyptsc (0.3 mM) in ethanol (10 mL) was added to a methanolic solution of $ZnCl_2$ (0.041 g, 0.3 mM; 10 mL). The reaction mixture was heated under reflux for 2 h and the off-white product was filtered off, washed with methanol, and dried in air.

2.2.4.1. *For [Zn(Hmpytsc)Cl_2].* Yield: 86%. Elemental Anal. Calcd $C_8H_{10}Cl_2N_4SZn$ (%): C, 29.2; Cl, 21.5; H, 3.0; N, 16.9; S, 9.7. Found (%): C, 29.1; Cl, 21.6; H, 2.8; N, 17.0; S, 9.4. Conductivity data (10^{-3} M in DMF): $\Lambda_M = 9.0\,\Omega^{-1}$. IR (Raman) cm^{-1}: 3347, $\nu_{as}(NH_2)$; 3254, $\nu_s(NH_2)$; 3156, ν(NH); 1619 (1636), ν(C=N); 1009 (1012) ν(N–N); 799 (787), ν(C=S); 621 (629), ρ(Py); 441 (445), ν(Zn–N); 317 (310), ν(Zn–S); 233 (252), ν(Zn–Cl) cm^{-1}; ^{1}H NMR (d_6-DMSO/TMS, ppm), δ: 8.07 (d, 1H, H_3); 7.70(t, 1H, H_4); 7.23 (d, 1H, H_5); 8.00 (s, 1H, H_7), 2.48 (s, 3H, CH_3); 11.63 (s, 1H, N(3)H); 8.13 (s, 1H, N(4)H_2); ^{13}C NMR (d_6-DMSO/TMS, ppm) δ: 158.2, C(2); 124.2, C(3); 137.7, C(4); 118.2, C(5); 153.2, C(6); 143.1, (CH=N); 178.9, (C=S); 24.4, 6-CH3.

2.2.4.2. *For [Zn(Hmpyptsc)Cl_2].* Yield: 88%. Elemental Anal. Calcd $C_{14}H_{14}Cl_2N_4SZn$ (%): C, 41.3; Cl, 17.5; H, 3.4; N, 13.8; S, 7.9. Found (%): C, 41.2; Cl, 17.5; H, 3.2; N, 13.6; S, 7.8. Conductivity data (10^{-3} M in DMF): $\Lambda_M = 8.0\,\Omega^{-1}$. IR (Raman) cm^{-1}: 3156,

Downloaded by [Institute Of Atmospheric Physics] at 15:20 09 December 2014

Downloaded by [Institute Of Atmospheric Physics] at 15:20 09 December 2014

ν(NH); 1619 (1636), ν(C=N); 1009 (1012), ν(N–N); 799 (787), ν(C=S); 621 (629), ρ(Py); 441 (445), ν(Zn–N); 317 (310), (Zn–S); 233 (252), ν(Zn–Cl); ^{1}H NMR (d_6-DMSO/TMS, ppm), δ: 8.27 (d, 1H, H_3); 7.81 (t, 1H, H_4); 7.55 (d, 1H, H_5); 8.13 (s, 1H, H_7); 2.50 (s, 3H, CH_3); 12.10 (s, 1H, N(3)H); 10.27 (s, 1H, N(4)H); 7.21–7.37(m, ph): ^{13}C NMR (d_6-DMSO/TMS, ppm) δ: 157.6, C(2); 125.7, C(3); 138.2, C(4); 118.5, C(5); 152.4, C(6); 142.8, (CH=N); 176.8, (C=S); 23.7, CH3; 123.3–139.3, Ph.

2.2.5. [Ru(PPh$_3$)$_2$L$_2$] (L = mpytsc, mpyptsc). Hmpytsc or Hmpyptsc (0.2 mM) in ethanol (10 mL) was added to solid [RuCl$_2$(PPh$_3$)$_3$] (0.1 g, 0.1 mM) and Et$_3$N (0.02 mL, 0.2 mM) was added. The reaction mixture was heated under reflux for 2 h. The yellow complex was filtered off warm, washed with hot ethanol, and air-dried.

2.2.5.1. *For [Ru(PPh$_3$)$_2$(mpytsc)$_2$].* Yield: 54%. Elemental Anal. Calcd $C_{52}H_{48}N_8P_2RuS_2$ (%): C, 61.7; H, 4.7; N, 11.1; S, 6.3. Found (%): C, 61.7; H, 4.5; N, 11.1; S, 6.1. Conductivity data (10^{-3} M in DMF): $\Lambda_M = 4.0\,\Omega^{-1}$. IR (Raman) cm^{-1}: 3306, ν_{as}(NH$_2$); 3281, ν_s(NH$_2$); 1635 (1587), ν(C=N); 1028 (1012), ν(N–N); 802 (809), ν(C=S); 622 (618), ρ(Py); 436 (438), ν(Ru–N), 325 (320), ν(Ru–S); ^{1}H NMR (d_6-DMSO/TMS, ppm), δ: 8.06 (d, 1H, H_3); 7.52 (t, 1H, H_4); 7.20 (d, 1H, H_5); 8.60 (s, 1H, H_7), 2.47 (s, 3H, CH_3); 6.67 (s, 2H, N(4)H$_2$); ^{13}C NMR (d_6-DMSO/TMS, ppm) δ: 159.3, C(2); 122.1, C(3); 137.7, C(4); 117.6, C(5); 155.5, C(6); 146.7, (CH=N); 173.5, (C=S); 24.5, 6-CH_3.

2.2.5.2. *For [Ru(PPh$_3$)$_2$(mpyptsc)$_2$].* Yield: 60%. Elemental Anal. Calcd $C_{64}H_{56}N_8P_2RuS_2$ (%): C, 66.0; H, 4.8; N, 9.6; S, 5.5. Found (%): C, 65.9; H, 4.5; N, 9.2; S, 5.5. Conductivity data (10^{-3} M in DMF): $\Lambda_M = 3.0\,\Omega^{-1}$. IR (Raman) cm^{-1}: 3270, ν(NH); 1592 (1599), ν(C=N); 999 (998), ν(N–N); 740 (742), ν(C=S); 644 (642), ρ(Py); 494 (475), ν(Ru–N); 344 (343), ν(Ru–S); ^{1}H NMR (d_6-DMSO/TMS, ppm), δ: 7.97 (d, 1H, H_3); 7.92 (t, 1H, H_4); 7.54 (d, 1H, H_5); 8.34 (s, 1H, H_7); 2.64 (s, 3H, CH_3); 10.24 (s, 1H, N(4)H); 7.20–7.42 (m, ph); ^{13}C NMR (d_6-DMSO/TMS, ppm) δ: 163.9, C(2); 124.4, C(3); 140.4, C(4); 120.6, C(5); 157.2, C(6); 152.6, (CH=N); 172.4, (C=S); 25.7, CH_3; 123.9–140.7, Ph.

2.2.6. [MLCl] (M(II) = Pd, Pt; L = mpytsc, mpyptsc). An aqueous solution of K_2PdCl_4 or K_2PtCl_4 (0.3 mM, 5 mL) was added to a methanolic solution of Hmpytsc or Hmpyptsc (0.3 mM) containing KOH (0.018 g, 0.3 mM; 15 mL). The reaction mixture was stirred at room temperature for 24 h. The orange precipitate was filtered off, washed with water and methanol, and air-dried.

2.2.6.1. *For [Pd(mpytsc)Cl].* Yield: 77%, Elemental Anal. Calcd $C_8H_9ClN_4PdS$ (%): C, 28.7; Cl, 10.6; H, 2.7; N, 16.7; Pd, 31.8; S, 9.6. Found (%): C, 28.6; Cl, 10.4; H, 2.4; N, 16.5; Pd, 31.5; S, 9.3. Conductivity data (10^{-3} M in DMF): $\Lambda_M = 12.0\,\Omega^{-1}$. IR (Raman) cm^{-1}: 3407, ν_{as}(NH$_2$); 3285, ν_s(NH$_2$); 1635 (1604), ν(C=N); 1003 (1001), ν(N–N); 780 (778), ν(C=S); 621 (621), ρ(Py); 438 (435), ν(Pd–N); 343 (340), ν(Pd–S); 315 (320), ν(Pd–Cl); ^{1}H NMR (d_6-DMSO/TMS, ppm), δ: 7.57 (d, 1H, H_3); 7.89 (t, 1H, H_4); 7.40 (d, 1H, H_5); 7.90 (s, 1H, H_7), 2.47 (s, 3H, CH_3); 7.80 (s, 2H, N(4)H$_2$); ^{13}C NMR (d_6-DMSO/TMS, ppm) δ: 163.5, C(2); 127.7, C(3); 140.6, C(4); 123.4, C(5); 157.7, C(6); 148.1, (CH=N); 172.1, (C=S); 24.7, 6-CH_3.

Downloaded by [Institute Of Atmospheric Physics] at 15:20 09 December 2014

2.2.6.2. *For [Pd(mpyptsc)Cl]*. Yield: 75%. Elemental Anal. Calcd $C_{14}H_{13}ClN_4PdS$ (%): C, 40.9; Cl, 8.6; H, 3.2; N, 13.6; Pd, 25.9; S, 7.80. Found (%): C, 40.9; Cl, 8.5; H, 3.1; N, 13.6; Pd, 25.9; S, 7.6. Conductivity data (10^{-3} M in DMF): $\Lambda_M = 10.0\,\Omega^{-1}$. IR (Raman) cm^{-1}: 3288, ν(NH); 1602 (1611), ν(C=N); 1006 (1007), ν(N–N); 752 (756), ν(N–N); 760 (683), ρ(Py); 439 (449), ν(Pd–N); 394 (391), ν(Pd–S); 271 (260), ν(Pd–Cl); ^{1}H NMR (d_6-DMSO/TMS, ppm), δ: 7.64 (d, 1H, H_3); 7.99(t, 1H, H_4); 7.65 (d, 1H, H_5); 7.28 (s, 1H, H_7) 2.48 (s, 3H, CH_3); 10.22 (s, 1H, N(4)H); 7.05–7.46 (m, ph); ^{13}C NMR (d_6-DMSO/TMS, ppm) δ: 166.6, C(2); 126.7, C(3); 142.7, C(4); 123.5, C(5); 161.5, C(6); 155.3, (CH=N); 171.3, (C=S); 28.1, CH_3; 126.2–142.9, Ph.

2.2.6.3. *For [Pt(mpytsc)Cl.* Yield: 62%. Elemental Anal. Calcd $C_8H_9ClN_4PtS$ (%): C, 22.6; Cl, 8.4; H, 2.1; N, 13.2; S, 7.6. Found (%): C, 22.4; Cl, 8.3; H, 2.0; N, 13.0; S, 7.5. Conductivity data (10^{-3} M in DMF): $\Lambda_M = 8.0\,\Omega^{-1}$. IR (Raman) cm^{-1}: 3300, $\nu_{as}(NH_2)$; 3258, $\nu_s(NH_2)$; 1599 (1615) ν(C=N); 1006 (1008), ν(N–N); 777 (779), ν(C=S); 686 (684), ρ(Py); 450 (455), ν(Pt–N); 359 (362), ν(Pt–S); 330 (334), ν(Pt–Cl); ^{1}H NMR (d_6-DMSO/TMS, ppm), δ: 7.59 (d, 1H, H_3); 7.97 (t, 1H, H_4); 7.45 (d, 1H, H_5); 8.42 (s, 1H, H_7), 2.49 (s, 3H, CH_3); 7.80 (s, 2H, N(4)H_2); ^{13}C NMR (d_6-DMSO/TMS, ppm) δ: 164.1, C(2); 128.9, C(3); 140.6, C(4); 123.5, C(5); 159.9, C(6); 148.5 (CH=N); 174.4 (C=S); 25.9, 6-CH_3.

2.2.6.4. *For [Pt(mpyptsc)Cl]*. Yield: 57%. Elemental Anal. Calcd $C_{14}H_{13}N_4PtS$ (%): C, 33.6; Cl, 7.1; H, 2.6; N, 11.2; S, 6.4. Found (%): C, 33.4; Cl, 7.0; H, 2.4; N, 11.4; S, 6.3. Conductivity data (10^{-3} M in DMF): $\Lambda_M = 7.0\,\Omega^{-1}$. IR (Raman) cm^{-1}: 3288, ν(NH); 1599 (1603), ν(C=N); 1009 (1112), ν(N–N); 742 (749), ν(C=S), 655 (652), ρ(Py); 453 (455), ν(Pt–N); 390 (391), ν(Pt–S); 295 (299), ν(Pt–Cl); ^{1}H NMR (d_6-DMSO/TMS, ppm), δ: 7.65 (d, 1H, H_3); 8.01 (t, 1H, H_4); 7.56 (d, 1H, H_5); 8.77 (s, 1H, H_7) 2.48 (s, 3H, CH_3); 10.28 (s, 1H, N(4)H); 7.037–7.53 (m, ph). ^{13}C NMR (d_6-DMSO/TMS, ppm) δ: 166.6, C(2); 126.7, C(3); 142.7, C(4); 123.5, C(5); 161.5, C(6); 155.3, (CH=N); 171.3, (C=S); 28.1, CH_3; 126.21–142.98, Ph.

2.3. *Biological assay*

The human colon cancer (HCT116) and prostate cancer (DU145) cells were maintained in Dulbecco's modified eagle medium (DMEM), containing 10% FBS, penicillin, fungizone, and streptomycin. Cells were maintained in an incubator with an atmosphere of 5% CO_2 at 37 °C. In all assays, drug stocks of 25 and 50 mM were prepared by dissolving in DMSO to ensure complete dissolution. The human colon cancer (HCT116) and prostate cancer (DU145) cells were grown to 80% confluence and then incubated in DMEM onto 96-well flat-bottomed micro-liter plates at a density of 5000 cells per well (100 µL/well) for 24 h at 37 °C. Subsequently, the cells were treated with Hmpytsc, Hmpyptsc, and their Zn(II), Pd (II), and Pt(II) complexes at decreasing concentrations. Drug stocks were diluted in DMEM supplemented with 10% FBS and antibiotics right before treatment. Cells in DMEM without drug treatment were included in each plate in triplicate as negative controls. Cells were fixed using 50 µL of cold trichloroacetic acid (50%) for 60 min at 4 °C, washed with water, stained with 0.4% sulforhodamine B for 4 h at room temperature, rinsed with 1% acetic acid, and allowed to dry overnight [19]. The resulting colored residue was dissolved in 200 µL Tris base (10 mM, pH 10.0) and optical density was recorded at 490 nm using a

microplate reader ELx808 (BioTek Instruments). The results were analyzed by Graph Pad Prism (Graph Pad Software, Inc., San Diego, CA), and the sigmoidal dose response curve was used to determine the 50% cell growth inhibitory concentration (IC_{50}). Each point represents the average of two independent experiments performed in triplicate [19].

3. Results and discussion

The Experimental section describes the modified synthesis method of 6-methylpyridine-2-carboxaldehydethiosemicarbazone (Hmpytsc) and 6-methylpyridine-2-carboxaldehyde-N(4)-phenylthiosemicarbazone (Hmpyptsc) [18], and their V(V), Zn(II), Ru(II), Pd(II), and Pt(II) complexes. Their elemental analyses are in excellent agreement with the assigned formulae. The molar conductivities (Λ_M) in DMF at room temperature suggest all complexes to be non-electrolytes [20]. [VO_2L] and [Zn(HL)Cl_2] were prepared from the addition of [VO_2(acac)$_2$] or $ZnCl_2$ to ligands in ethanol or methanol, respectively. On the other hand, [Ru(PPh_3)$_2$$L_2$] and [MLCl] (M(II) = Pd, Pt) were obtained from the reaction of [Ru(PPh_3)$_2$$Cl_2$] or K_2MCl_4 and ligands in ethanol or aqueous methanol under basic conditions. All the reported complexes are microcrystalline or powder-like, stable under normal laboratory conditions, and soluble in DMF, DCM, and DMSO.

Orange needles, suitable for X-ray crystallography, were obtained by slow evaporation of a solution of [Pd(mpyptsc)Cl] in DMSO-DCM (1 : 1) at room temperature. These crystals were mounted on the diffractometer and the unit-cell dimensions and intensity data were

Table 1. Crystal data and structure refinement of [Pd(mpyptsc)Cl]·DMSO.

Empirical formula	$C_{16}H_{19}ClN_4OPdS_2$
Formula weight	489.32
Temperature	200 K
Wavelength	1.54178 Å
Crystal system	Monoclinic
Space group	$P2_{1/c}$
Unit-cell dimensions	$a = 7.2407(2)$ Å, $\alpha = 90°$ $b = 11.1883(3)$ Å, $\beta = 97.850(2)°$ $c = 23.5428(6)$ Å, $\gamma = 90°$
Volume	1889.36(9) Å^3
Z	4
Density (Calcd)	1.720 g cm^{-3}
Absorption coefficient	11.396 mm^{-1}
F(0 0 0)	984
Crystal size	0.16 × 0.08 × 0.04 mm
θ Range for data collection	3.79–71.94
Index ranges	$-8 \le h \le 8$, $-13 \le k \le 13$, $-28 \le l \le 28$
Reflections collected	23,587
Independent reflections	3672 ($R_{int} = 0.055$)
Absorption correction	Semi-empirical from equivalents
Max. and min. transmission	0.6339 and 0.3716
Refinement method	Full-matrix least-squares on F^2
Data/restraints/parameters	3672/0/233
Goodness-of-fit on F^2	1.024
Final R indices [$I > 2\sigma(I)$]	$R_1 = 0.0366$, $wR_2 = 0.0931$
R indices (all data)	$R_1 = 0.0514$, $wR_2 = 0.1042$
Largest diff. peak and hole	1.077 and −0.907 e Å^{-3}

Downloaded by [Institute Of Atmospheric Physics] at 15:20 09 December 2014

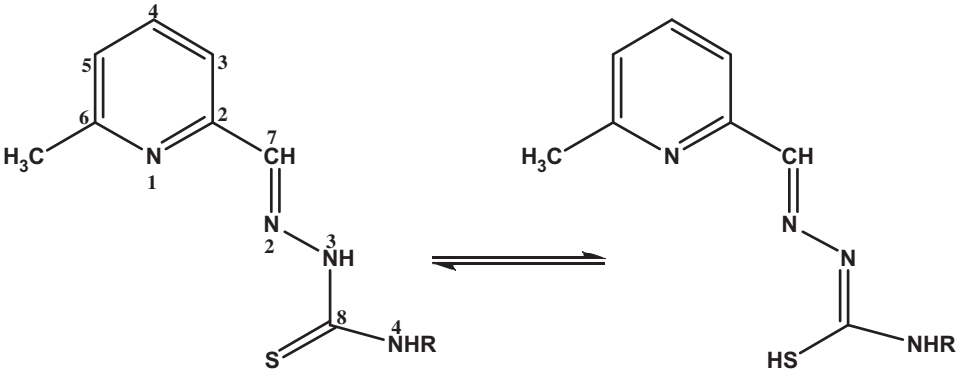

Figure 1. Tautomeric forms of 6-methylpyridine-2-carbaldehydethiosemicarbazone (R = H, Hmpytsc) and 6-methylpyridine-2-carbaldehyde-N(4)-phenylthiosemicarbazone (R = Ph, Hmpyptsc).

measured at 200 K. The structure was solved by least-squares fit of the angular setting of strong reflections based on F^2. The relevant crystal data and experimental conditions along with the final parameters are summarized in table 1.

3.1. *Vibration spectra*

We reported earlier the vibrational spectroscopic data of 2-formylpyridinethiosemicarbazone, 6-methylpyridine-2-carbaldehyde-N(4)-ethylthiosemicarbazone, and a number of their complexes [8, 9]. The characteristic IR and Raman bands observed for 6-methylpyridine-2-carboxaldehydethiosemicarbazone (Hmpytsc) and 6-methylpyridine-2-carboxaldehyde-N(4)-phenyl thiosemicarbazone (Hmpyptsc), and their new complexes, together with the proposed vibrational assignments, are presented in the Experimental section and they are in good agreement with the data reported earlier [18]. Hmpytsc and Hmpyptsc have the thioamide moiety [–NH–C(=S)–NH_2], which exhibits thione–thiol tautomerism (figure 1) [8, 9, 18, 21]. The absence of ν(SH) band at ca. 2600 cm^{-1} indicates that Hmpytsc and Hmpyptsc are predominantly in the thione form in the solid state [8, 9, 21, 22]. In solution and in the presence of metal ions, however, it may convert to the deprotonated thiol form [8, 9, 21]. The spectra of the free Hmpytsc and Hmpyptsc exhibit strong IR bands at 1612 and 1588 cm^{-1} (1608 and 1606 cm^{-1} in Raman), respectively, which is characteristic for ν(HC=N). The coordination of the azomethine N to the metal ion reduces the electron density in its link, and thus shifts its stretch to lower wavenumbers [8, 9, 23]. In the complexes, this band is observed at 1635–1599 cm^{-1}, supporting coordination through the azomethine N [8, 9, 24]. The band near 3150 cm^{-1} in the free ligands (near 3100 cm^{-1} in Raman), arising from ν(NH), is not observed in the complexes [25]. The ν(C=S) stretches at 842 and 784 cm^{-1} (at 799 and 792 cm^{-1} in Raman) in free Hmpytsc and Hmpyptsc, respectively, are less intense in the V(V), Pd(II), and Pt(II) complexes and shifted to lower frequency, suggesting coordination of the metal through sulfur. The coordination of the thiolato sulfur was further indicated by a decrease in the energy of the thioamide band as well as by the presence of a band near 350 cm^{-1} assigned to ν(M–S) [26]. In spectra of Hmpytsc, bands at 3392 and 3258 cm^{-1} assigned to $\nu_{as}(NH_2)$ and $\nu_s(NH_2)$ stretches, respectively, are shifted to

Downloaded by [Institute Of Atmospheric Physics] at 15:20 09 December 2014

Downloaded by [Institute Of Atmospheric Physics] at 15:20 09 December 2014

lower wavenumbers upon complex formation [8, 9, 12]. The free ligands show an intense band near 992 cm^{-1} assigned to ν(N–N), which shifted to higher frequency in the complexes [8, 9]. Furthermore, the pyridine ring deformation mode at 562 cm^{-1} in the free ligands is shifted to near 590 cm^{-1} in the complexes, indicating participation of pyridyl N in coordination [8, 9]. The significant changes in the ligand bands upon complexation are the decrease in ν(C=N), increase in ν(N–N), and the absence of large systematic shifts of $\nu_{as}(NH_2)$ to lower frequencies (in case of mpytsc complexes). These data indicate coordination through azomethine nitrogen without interaction between the terminal amino nitrogen and the metal ion. The IR and Raman data suggest mono-negative tridentate N,N,S^- coordination of $mpytsc^-$ and $mpyptsc^-$ to the metal ions. In the case of $[Zn(HL)Cl_2]$ (HL = Hmpytsc, Hmpyptsc), ν(NH) is shifted to lower wavenumbers since the thione S is taking part in coordination. Also, the pyridine ring deformation mode is observed more or less in the same position in the free ligands near 560 cm^{-1}, i.e. Hmpytsc and Hmpyptsc are neutral bidentate ligands through azomethine N and thione S [7–9]. The spectra of the Ru (II) complexes show shifts of ν(HC=N) to 1635 and 1592 cm^{-1} in IR (1587 and 1599 cm^{-1} in Raman), while the ν(C=S) stretch shifts to lower energy (802 and 740 cm^{-1} in IR, and 890 and 747 cm^{-1} in Raman) for $[Ru(mpytsc)(PPh_3)_2]$ and $[Ru(mpyptsc)(PPh_3)_2]$, respectively [8, 9]. Moreover, ν(N–N) shifts to higher energies while there is no shift observed in the pyridyl ring deformation mode. These features support the mono-negative bidentate coordination of the $mpytsc^-$ and $mpyptsc^-$ to Ru(II) through the azomethine N and thiolato S [7–9, 27].

As expected, the presence of coordinated PPh_3 in $[RuL_2(PPh_3)_2]$ is manifested by strong IR bands near 1100 and 750 cm^{-1}, attributed to the ν(P–C) and δ(C–CH) vibrations, respectively [28]. The spectra of $[VO_2L]$ show two extra IR bands characteristic of the *cis*-VO_2 core near 935 and 910 cm^{-1} (near 940 and 900 cm^{-1} in Raman) assigned to ν_{as}(O=V=O) and ν_s(O=V=O) stretches, respectively [9]. Finally, extra-far IR and Raman bands are observed near 450, 350, and 280 cm^{-1}, attributed to ν(M–N), ν(M–S), and ν(M–Cl) stretches, respectively [7–10, 28, 29].

3.2. *NMR spectra*

The ^{1}HNMR spectral data of Hmpytsc, Hmpyptsc, and their metal complexes (in d_6-DMSO) are listed in the Experimental section (see figure 1 for numbering scheme); they are in agreement with those reported earlier [18]. The spectra of free Hmpytsc and Hmpyptsc exhibit singlets at δ 11.61 and 12.01 ppm, respectively, assigned to N(3)H. This signal is missing in the complexes, indicating coordination of the deprotonated thiol S to the central metal ions [8, 9]. As expected, in $[Zn(HL)Cl_2]$ complexes, this signal is observed at δ 11.63 (Hmpytsc) and 12.100 (Hmpyptsc) ppm, confirming the coordination of thione S to Zn(II) [7–9]. The singlet at δ 8.01 and 8.13 ppm in free Hmpytsc and Hmpyptsc, respectively, arising from the azomethine CH(7)=N proton is shifted downfield in the complexes due to the involvement of azomethine N in coordination [7]. In Hmpytsc, the two hydrogens in the terminal nitrogen, $N(4)H_2$, are not equivalent and are assigned to a pair of singlets at δ 8.12 and 8.13 ppm, indicating restricted rotation about the S=C-NH_2 group; these signals are shifted upfield upon complex formation [11]. In the spectrum of Hmpyptsc, the N(4)H proton shows a singlet at δ 10.29 ppm, which is also shifted upfield in the complexes. The 6-CH_3 and pyridine protons appear near δ 2.45 and 7.202–8.190 ppm, respectively. In the complexes, the pyridine ring protons are shifted downfield, except in case of

Downloaded by [Institute Of Atmospheric Physics] at 15:20 09 December 2014

$[Zn(HL)Cl_2]$, due to the decrease in the electron density caused by electron withdrawal by the metal ions from pyridyl N [14, 30]. ^{13}C NMR spectral data of Hmptsc, Hmpyptsc, and their complexes are reported in the Experimental section. It is clear that the resonances of carbons adjacent to the coordination centers in the complexes, i.e. C(2), C(6), and C(7) shift downfield relative to their positions in the free ligands [8, 9, 31]. In the free ligands, the C=S resonance is observed near 177.0 ppm, which is shifted upfield 3–5 ppm in the complexes, attributed to the complexation through sulfur, which apparently is related to an increased electron density at this site, probably due to π-back bonding for thiolato S [32]. This feature is due to the increase in current brought about by coordination to pyridyl N, azomethine N, and deprotonated thiol S [8, 9]. In spectra of $[Zn(HL)Cl_2]$ and $[RuL_2(PPh_3)_2]$, the resonances arising from C(6) and C(2) are more or less in the same positions as in the free ligands, confirming coordination of Hmpytsc and Hmpyptsc to Zn(II) or Ru(II) through thione S (Zn(II)) and thiolato S^- (Ru(II)), and azomethine N without any participation of the pyridyl N in coordination [8, 9].

^{31}PNMR spectra of $[Ru(PPh_3)_2L_2]$ show sharp singlets at δ 52.34 (Hmpytsc) and 56.2 (Hmpyptsc) ppm. The observation of only one signal in the spectra of the complexes suggests that the two triphenylphosphine groups are magnetically equivalent [33].

3.3. *Mass spectra*

The mass spectrum of Hmpytsc ($C_8H_{10}N_4S$) is in agreement with the assigned formula {*m*/e 194.0 (Calcd 194.0)} with 100% abundances. Three more signals are observed at 134, 106, and 93 corresponding to $C_7H_8N_3$ (Calcd 134.0), C_7H_8N (Calcd 106), and C_6H_7N (Calcd 93) fragments, respectively. The spectrum of Hmpyptsc ($C_{14}H_{14}N_4S$) shows a peak at *m*/*e* 270.9 (Calcd 270.0) with 16% abundance. The peak at 178.8 (Calcd 178.0) corresponds to $C_8H_8N_3S$ fragment.

The mass spectra of the complexes were measured and their molecular ion peaks are in agreement with their calculated formulas. In the spectra of $[Ru(L)_2(PPh_3)_2]$ (L = mpytsc, mpyptsc), the peaks at *m*/*z* 1011.8 (Calcd 1011.1) and 1164.0 (Calcd 1163.1) with 31 and 42% abundance are assigned to the molecular ions $[Ru(mpytsc)_2(PPh_3)_2]^+$ and $[Ru(mpyptsc)_2(PPh_3)_2]^+$, respectively. The fragmentation patterns indicate the stepwise L^- and PPh_3 ligand loss. Three more fragments for mpystc, $[Ru(mpytsc)(PPh_3)_2]^+$ (818.8), $[Ru(mpystc)(PPh_3)]^+$ (557.1), and $[Ru(PPh_3)]^+$ (363.5); while for mpyptsc two more fragments, $[Ru(mpyptsc)_2(PPh_3)]^+$ (902.2) and $[Ru(PPh_3)]^+$ (363.9), were obtained [34]. The mass spectra of $[VO_2L]$ (L = mpytsc, mpyptsc) show signals at *m*/*z* 277.3 (Calcd 276.0) and 351.0 (Calcd 351.9) with 89 and 82% abundance, corresponding to $[VO_2(mpytsc)]^+$ and $[VO_2(mpyptsc)]^+$, respectively. In the latter complex, three more peaks are observed at 286.0, 255.0, and 241.2 corresponding to $[VO_2(mpyptsc\text{-}C_5H_6)]^+$, $[VO_2(mpyptsc\text{-}C_5H_6S)]^+$, and $[VO_2(mpyptsc\text{-}C_6H_6NS)]^+$, respectively. The spectrum of [Pt(mpytsc)Cl] displays a signal at 423.9 (Calcd 423.5) with 8% abundance, assigned to $[Pt(mpyptsc)Cl]^+$. The fragmentation pattern shows the loss of Cl at 387.2 (Calcd 388.0). The mass spectrum of $[Zn(Hmpyptsc)Cl_2]$ shows a signal at 406.0 (Calcd 406.5) with 46% abundance, corresponding to $[Zn(Hmpyptsc)Cl_2]^+$. The fragmentation pattern indicates the loss of Cl_2 [35] and C_4H_5 fragments at 282.0 (Calcd 282.5).

Downloaded by [Institute Of Atmospheric Physics] at 15:20 09 December 2014

3.4. *Electronic spectra*

The UV–vis spectra of Hmpytsc, Hmpyptsc, and their complexes were recorded in DMF. The absorptions in the UV region are due to transitions within ligand orbitals, while those in the visible region are assigned to transitions involving both metal and ligand orbitals [36]. The spectra of Hmpytsc and Hmpyptsc show broadbands in the 290–360 nm region, attributable to n–π^* transitions of the pyridine and phenyl rings, as well as azomethine and thioamide moieties [18, 37]. The electronic spectra of the diamagnetic Ru(II) complexes show three bands near 500, 390, and 340 nm corresponding to $^1A_{1g} \rightarrow {}^1T_{1g}$, $^1A_{1g} \rightarrow {}^1T_{2g}$, and ligand (p-dp) transitions, respectively [8, 10, 12]. These transitions are attributed to a low-spin octahedral geometry around Ru(II) [10]. The electronic spectra of the diamagnetic Pd(II) and Pt(II) complexes exhibit two absorptions near 380 and 465 nm, assigned to $^1A_{1g} \rightarrow {}^1B_g$ and $^1A_{1g} \rightarrow {}^1E_g$ transitions, respectively, confirming square-planar geometry [11–15].

3.5. *X-ray crystallography*

Orange needles, suitable for X-ray crystallography of [Pd(mpyptsc)Cl]·DMSO, were obtained from slow evaporation of a solution of [Pd(mpyptsc)Cl] in DMSO-DCM (1 : 1). These crystals crystallize in a monoclinic lattice with space group symmetry $P_{21/c}$. The crystal data and structure refinement details are given in table 1.

The structure and atomic labeling are shown in figure 2. The complex is planar except for the phenyl group, which is twisted out of the plane by 10.5°. The square-planar palladium coordinates the pyridyl nitrogen N(1), the azomethine nitrogen N(7), and thiolato sulfur of mpyptsc$^-$ in a ZEZ configuration. The fourth coordination site is occupied by a chloride. The coordinated ligand consists of heterocyclic, PdNCCN, and PdNNCS rings.

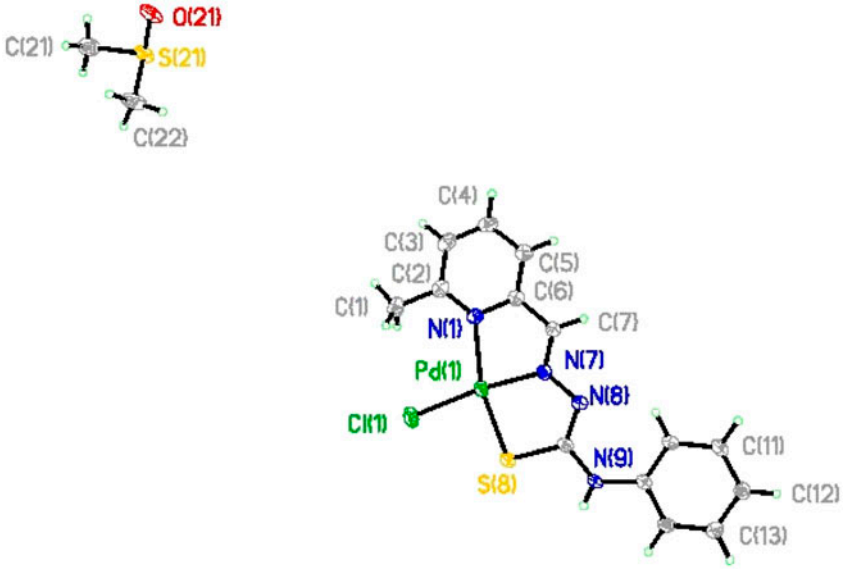

Figure 2. X-ray crystal structure of [Pd(mpyptsc)Cl]·DMSO.

Table 2. Selected bond lengths (Å) and angles (°) of [Pd(mpyptsc)Cl)]·DMSO.

Bond lengths		Bond angles	
Pd(1)–N(7)	1.970(3)	N(7)–Pd1–N(1)	80.34(13)
Pd(1)–N(1)	2.171(3)	N(7)–Pd1–S(8)	83.59(10)
Pd(1)–S(8)	2.2421(11)	N(1)–Pd1–S(8)	163.84(10)
Pd(1)–Cl(1)	2.3238(11)	N(7)–Pd1–Cl1	172.83(10)
S(8)–C(8)	1.774(4)	N(1)–Pd1–Cl1	106.77(10)
N(1)–C(2)	1.335(5)	S(8)–Pd1–Cl1	89.34(4)
N(1)–C(6)	1.375(5)	C(8)–S(8)–Pd1	96.08(14)
N(7)–C(7)	1.295(5)	C(2)–N(1)–C(6)	118.5(4)
N(7)–N(8)	1.372(4)	C(2)–N(1)–Pd1	133.6(3)
N(8)–C(8)	1.308(5)	C(6)–N(1)–Pd1	107.9(3)
N(9)–C(8)	1.352(5)	C(7)–N(7)–N(8)	118.8(3)
N(9)–C(9)	1.414(5)	C(7)–N(7)–Pd1	116.6(3)
S(21)–O(21)	1.509(4)	N(8)–N(7)–Pd1	124.6(3)
(21)–C(22)	1.763(5)	C(8)–N(8)–N(7)	111.7(3)
S(21)–C(21)	1.771(5)	C(8)–N(9)–C(9)	129.9(3)
		N(1)–C(2)–C(3)	120.5(4)
		N(1)–C(2)–C(1)	119.4(4)
		N(8)–C(8)–S(8)	124.0(3)
		N(8)–C(8)–N(9)	121.0(4)
		N(9)–C(8)–S(8)	115.0(3)
		C(13)–C(14)–C(9)	121.6(4)
		O(21)–S(21)–C(22)	106.1(3)
		O(21)–S(21)–C(21)	106.3(3)
		C(22)–S(21)–C(21)	97.2(3)

Selected bond angles (°) and bond lengths (Å) are listed in table 2. The bond lengths and angles of the phenyl and pyridyl rings are normal. The bite angles N(1)–Pd–N(7), 80.34 (13)°; N(7)–Pd–S, 83.59(10)°; N(1)–Pd–Cl, 106.77(10)°; and S–Pd–Cl, 89.34(4)°, and the bond lengths of Pd–N(1), Pd–N(7), Pd–S, and Pd–Cl are 2.171(3), 1.970(3), 2.2421(11), and 2.3238(11) Å, longer than those reported for square-planar Pd(II) complexes with N,N, S-donors [38] and similar to [Pd(fpytsc)X] (Hfpytsc = 2-formylpyridinethiosemicarbazone; X = CN, PPh_3) and [Pt(mpyetsc)Cl] (Hmpyetsc = 6-methylpyridine-2-carbaldehyde-N(4)-ethylthiosemicarbazone) complexes, which we have reported earlier [8, 9]. The bond length of Pd–N(1), 2.171(3) Å is longer than that of Pd–N(7), 1.970(3) Å; the weak coordination of Pd(II) to the pyridyl nitrogen N(1) compared to azomethine N(7) is attributed to high basicity of the latter [8, 9]. The bond distance, C(8)–S, 1.774(4) Å is intermediate between C=S double bond (1.62 Å) and C–S single bond (1.82 Å), i.e. C(8)–S suggesting partial single-bond character [8, 9, 32, 38]. In addition, the bond lengths of C(8)–N(8), 1.308(5) Å, and C(7)–N(7), 1.295(5) Å, are close to a double bond (1.28 Å), while that of N(7)–N(8), 1.372(4) Å, is very close to a single bond [8, 9, 32]. The S–C bond distances are consistent with increased single-bond character, while both thioamide C–N distances indicate increased double-bond character. The negative charge of the deprotonated ligand is delocalized over the thiosemicarbazonate. This is indicative of the coordinated thiosemicarbazone's

Table 3. Bond lengths (Å) and angles (°) related to the hydrogen bonding for [Pd(mpyptsc)Cl)]·DMSO.

D–H	…A	d(D–H)	d(H…A)	d(D…A)	∠DHA
N(9)–H(9)	O(21)#1	0.77(5)	2.08(5)	2.840(5)	169(4)

Downloaded by [Institute Of Atmospheric Physics] at 15:20 09 December 2014

greater conjugation and more delocalized electron density [32]. The bond angles, N(7)–Pd–Cl, 172.83(10)°, and N(1)–Pd–S, 163.84(10)°, deviate substantially from that expected for regular square-planar geometry [8, 9].

The complex molecules are linked through intermolecular hydrogen bonds. The monomers form hydrogen-bonded dimers linked by Ph–N(9)–H and DMSO–O(21). The observed hydrogen bonding patterns are of the DH and DA [32]. Table 3 shows bond lengths and angles related to the hydrogen bonding of the dimeric complex.

3.6. *DFT computation study*

The structure of Pd(mpyptsc)Cl as well as both thione and thiol forms of Hmpyptsc (figure 1) were calculated using the Gaussian 03 Rev B-02 programs [17]. The geometry optimization was carried out using the DFT computational method with the DGDZVP/B3LYP basis set. [Pd(mpyptsc)Cl] was found to be planar with all dihedral angles within 2° of 0° or 180° except for the phenyl ring which is twisted out of plane by 10.5° in the crystal structure data and 37.6° (in calculation) (figure 3). In the thiol and thione forms of Hmpyptsc, the angle is 29° and 38°, respectively. This difference is presumably due to crystal packing forces. The calculated bond lengths and angles are in agreement with the experimental values. Figure 3 shows the calculated structures of [Pd(mpyptsc)Cl], $Hmpyptsc_{thione}$ and $Hmpyptsc_{thiol}$. The distances between N(1) and N(9) are 6.059, 6.292, and 6.342 Å, respectively. Thus, the basic structure of Hmpyptsc changes little upon coordination, and the geometry around palladium is constrained by the rigidity of the ligand, accounting for the

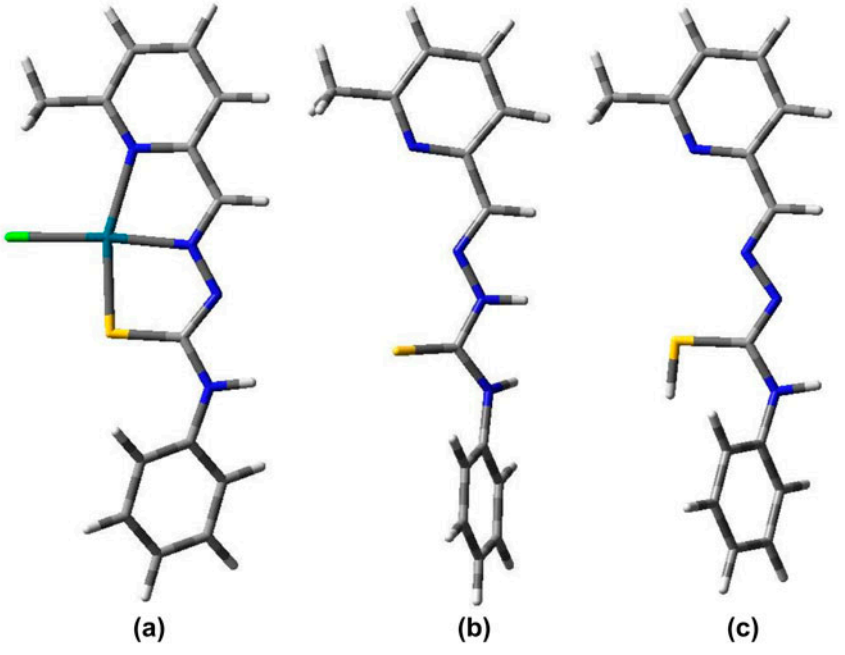

Figure 3. The calculated geometries of (a) [Pd(mpyptsc)Cl], (b) Hmpyptsc in thione, and (c) thiol tautomeric forms.

Downloaded by [Institute Of Atmospheric Physics] at 15:20 09 December 2014

distorted geometry. Free Hmpyptsc is more stable in the thione form than the thiol one (figures 1 and 3) by 9.54 kJ M^{-1} [35].

3.7. *Biological applications*

Cisplatin is one of the best-known small metal-containing drug molecules. It acts as an anticancer agent for several human cancers, particularly testicular and ovarian cancers [11]. Generally, the side effects, especially nephrotoxicity, limit its widespread use in high doses [39]. The need to develop new complexes with reduced nephrotoxicity and higher activity has stimulated the synthesis of many new complexes. Over the past years, a renewed interest in Zn(II), Pd(II), Ag(I), and Pt(II) complexes as potential anticancer agents has developed in our laboratory [9–15, 40].

The ultimate goal of this research is to develop new complexes with high efficacy against cancer cells. Free Hmpytsc and Hmpyptsc (HL), and their complexes, [Zn(HL)Cl_2], [Pd(L)Cl], and [Pt(L)Cl], were evaluated *in vitro* for their inhibitory effects on cell growth proliferation of human colon cancer (HCT116) and prostate (DU145) cell lines in comparison to cisplatin as a reference (figure 4).

The cell growth proliferation was evaluated by DMEM assay. The final IC_{50} values for cell growth proliferation after 24 h of incubation with free Hmpytsc and Hmpyptsc, and their complexes, [Zn(Hmpytsc)Cl_2], [Zn(Hmpyptsc)Cl_2], [Pd(mpytsc)Cl], [Pd(mpyptsc)Cl],

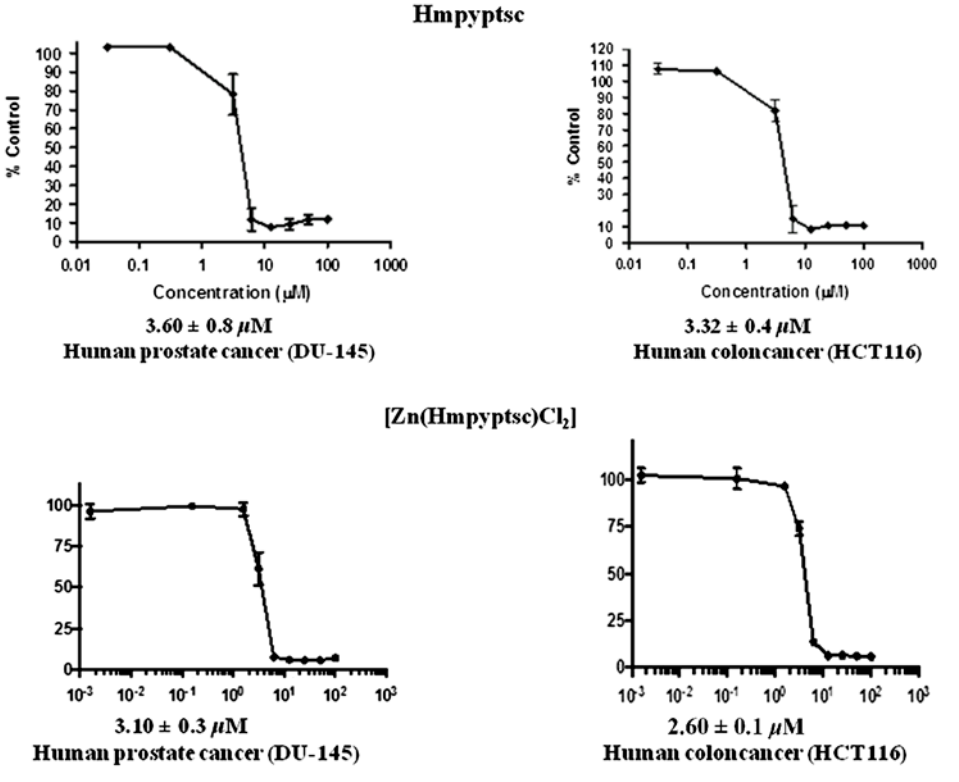

Figure 4. Anticancer activity of Hmpyptsc and [Zn(Hmpyptsc)Cl_2] against human colon cancer (HCT116) and human prostate (DU145) cell line.

Downloaded by [Institute Of Atmospheric Physics] at 15:20 09 December 2014

Downloaded by [Institute Of Atmospheric Physics] at 15:20 09 December 2014

[Pt(mpytsc)Cl], and [Pt(mpyptsc)Cl], for human colon cancer (HCT116) cells were >100, 3.3 ± 0.4, 84.8 ± 0.3, 2.6 ± 0.1, 46.0 ± 0.2, 38 ± 1, 87 ± 1, and 84 ± 1 μM, respectively. For prostate colon cancer (DU145), cells were >100, 3.6 ± 0.8, >100, 3.1 ± 0.3, 87.5 ± 0.8, 46 ± 1, >100, and 93.5 ± 0.6 μM, respectively. The IC_{50} values of cisplatin are 18.0 ± 0.4 (HCT116) and 22.5 ± 0.7 (DU145) μM. Thus, the order for cytotoxic activity of the drugs is [Zn(Hmpyptsc)Cl_2] > Hmpyptsc > [Pd(mpyptsc)Cl] > [Pd(mpytsc)Cl] > [Pt(mpyptsc)Cl] > [Zn(Hmpytsc)Cl_2] > [Pt(mpytsc)Cl]. We previously reported the *in vitro* anticancer activity of 6-methylpyridine-2-carbaldehyde-N(4)-ethylthiosemicarbazone (HmpETSC) and its complexes, [Zn(HmpETSC)Cl_2] and [M(mpETSC)Cl] (M(II) = Pd, Pt), against human colon cancer (HCT116) cell line [9]. Generally, nitrogen-containing ligands have important effects on cytotoxicity [41]. [Zn(HmpETSC)Cl_2] exhibits higher anticancer activity compared to [Pd(mpETSC)Cl], which is more active than its Pt(II) analog. Generally, substituted groups as well as the modes of chelation of HmpETSC in the complexes may play a role in their anticancer activity towards human cancer cell lines [9, 41, 42]. An important aspect of the anticancer activity of [Zn(Hmpyptsc)Cl_2] is the high degree of conjugation of the (–CH=N–N–C(=S)–NH(Ph)) moiety, i.e. phenyl when compared to its ethyl analog in [Zn(HmpETS)Cl_2] [28, 43]. Generally, the Zn(II) complexes show higher activity than their free ligands, as a result of the polarity reduction of the complex molecule as a whole, when compared with the free ligand, by partial sharing of their charges within the coordination compounds, favoring their permeation through the cell membrane, hence resulting in a better cell uptake of the active species [44].

Cepeda *et al.* reported that the binding of cisplatin to genomic DNA (gDNA) in the cell nucleus is the main event responsible for its antitumor properties [45]. Thus, the damage induced upon binding of cisplatin to gDNA may inhibit transcription and/or DNA replication mechanisms. Subsequently, these alterations in DNA processing would trigger cytotoxic processes that lead to cancer cell death. An important property of the complexes is the ligand exchange process. The low activity of [Pd(mpyptsc)Cl] may be due to the poor solubility, difficulty in hydrolysis to produce their cationic form, fast interaction with DNA under physiological conditions [46], or the presence of intermolecular hydrogen bonds, as indicated from the crystal structure of [Pd(mpyptsc)Cl] [15].

4. Conclusion

The new complexes, [VO_2L], [Zn(HL)Cl_2], [Ru(PPh_3)$_2$$L_2$], and [MLCl] (M(II) = Pd, Pt; HL = 6-methylpyridine-2-carbaldehydethiosemicarbazone (Hmpytsc), 6-methylpyridine-2-carbaldehyde-N(4)-phenylthiosemicarbazone (Hmpyptsc)), were prepared and characterized. In the complexes, [VO_2L] and [MLCl] (M(II) = Pd, Pt), mpytsc$^-$ and mpyptsc$^-$ are mono-anionic tridentate ligands bonding through pyridyl N, azomethine N, and thiolato S; for [Zn(HL)Cl_2], they function as neutral bidentate through azomethine N and thione S. In addition, they are mono-negative bidentate through azomethine N and thiolato S for [Ru(PPh_3)$_2$$L_2$]. The X-ray crystal structure and DFT conformational analysis of [Pd(mpyptsc)Cl]·DMSO were discussed. [Pd(mpyptsc)Cl]·DMSO shows Pd(II) ion in a distorted square plane, ligated by mono-anionic tridentate, pyridyl N, azomethine N, and thiolato S of mpyptsc$^-$ moiety, and chloride. Free Hmpyptsc and [Zn(Hmpyptsc)Cl_2] exhibit the highest growth inhibitor activity against human colon cancer (CHT116) and prostate cancer (DU145) with mean IC_{50} values of 3.32 and 2.60 (HCT116), and 3.60 and 3.10 (DU145) μM, respectively.

CCDC numbers

CCDC number of the crystal obtained of [Pd(mpyptsc)Cl]·DMSO is 866624.

Acknowledgements

We are grateful to the Ministry of Higher Education in Egypt (E.S.) and NSERC (Canada) Discovery grant (ISB) for the financial support of this work. We would also like to thank Prof. M.A. Whitehead and Mr K. Conley for helpful discussions.

Downloaded by [Institute Of Atmospheric Physics] at 15:20 09 December 2014

Supplemental data

Supplemental data for this article can be accessed here [http://dx.doi.org/10.1080/00958972.2014.942224]

References

[1] V.B. Arion, M.A. Jakupec, M. Galanski, P. Unfried, B.K. Keppler. *J. Inorg. Biochem.*, **91**, 298 (2002).
[2] C.C. Garcia, B.N. Brousse, M.J. Carlucci. *Antiviral Chem. Chemother.*, **14**, 99 (2003).
[3] W.X. Hu, W. Zhou, C.N. Xia, X. Wen. *Bioorg. Med. Chem. Lett.*, **16**, 2213 (2006).
[4] E.M. Jouad, G. Larcher, M. Allain. *J. Inorg. Biochem.*, **86**, 565 (2001).
[5] A. Gölcü, M. Dolaz, H. Demirelli, M. Diðrak, S. Serin. *Transition Met. Chem.*, **31**, 658 (2006).
[6] E.J. Blanz Jr, F.A. French. *Cancer Res.*, **28**, 2419 (1968).
[7] S.I. Mostafa, A.A. El-Asmy, S.M. El-Shahawy. *Transition Met. Chem.*, **25**, 470 (2000).
[8] S.A. Elsayed, A.M. El-Hendawy, S.I. Mostafa, I.S. Butler. *Inorg. Chim. Acta*, **363**, 2526 (2010).
[9] S.A. Elsayed, A.M. El-Hendawy, S.I. Mostafa, B.J. Jean-Claude, M. Todorova, I.S. Butler. *Bioinorg. Chem. Appl.*, **2010**, Article ID 149149, 11 (2010). doi:10.1155/2010/149149.
[10] S.I. Mostafa. *J. Coord. Chem.*, **61**, 1553 (2008).
[11] S.I. Mostafa, F.A. Badria. *Met.-Based Drugs*, **2008**, Article ID 723634, 7 (2008). doi:10.1155/2008/723634.
[12] I. Gabr, H. El-Asmy, M. Emmam, S.I. Mostafa. *Transition Met. Chem.*, **34**, 409 (2009).
[13] S.I. Mostafa. *Transition Met. Chem.*, **32**, 769 (2007).
[14] S.A. Elsayed, B.J. Jean-Claude, I.S. Butler, S.I. Mostafa. *J. Mol. Struct.*, **1028**, 208 (2012).
[15] A.A. Alie El-Deen, A.E. El-Askalany, R. Halaoui, B.J. Jean Claude, I.S. Butler, S.I. Mostafa. *J. Mol. Struct.*, **1036**, 161 (2013).
[16] T.A. Stephenson, G. Wilkinson. *J. Inorg. Nucl. Chem.*, **28**, 945 (1966).
[17] M.J. Frisch, G.W. Trucks, H.B. Schlegel, G.E. Scuseria, M.A. Robb, J.R. Cheeseman Jr, J.A. Montgomery, T. Vreven, K.N. Kudin, J.C. Burant, J.M. Millam, S.S. Iyengar, J. Tomasi, V. Barone, B. Mennucci, M. Cossi, G. Scalmani, N. Rega, G.A. Petersson, H. Nakatsuji, M. Hada, M. Ehara, K. Toyota, R. Fukuda, J. Hasegawa, M. Ishida, T. Nakajima, Y. Honda, O. Kitao, H. Nakai, M. Klene, X. Li, J.E. Knox, H.P. Hratchian, J.B. Cross, C. Adamo, J. Jaramillo, R. Gomperts, R.E. Stratmann, O. Yazyev, A.J. Austin, R. Cammi, C. Pomelli, J.W. Ochterski, P.Y. Ayala, K. Morokuma, G.A. Voth, P. Salvador, J.J. Dannenberg, V.G. Zakrzewski, S. Dapprich, A.D. Daniels, M.C. Strain, O. Farkas, D.K. Malick, A.D. Rabuck, K. Raghavachari, J.B. Foresman, J.V. Ortiz, Q. Cui, A.G. Baboul, S. Clifford, J. Cioslowski, B.B. Stefanov, G. Liu, A. Liashenko, P. Piskorz, I. Komaromi, R.L. Martin, D.J. Fox, T. Keith, M.A. Al-Laham, C.Y. Peng, A. Nanayakkara, M. Challacombe, P.M.W. Gill, B. Johnson, W. Chen, M.W. Wong, C. Gonzalez, J.A. Pople. *Gaussian 03, Revision B.02*, Gaussian, Inc., Pittsburgh, PA (2003).
[18] (a) D.X. West, S.L. Dietrich, I. Thientanavanich, C.A. Brown, A.E. Liberta. *Transition Met. Chem.*, **19**, 195 (1994); (b) F.C. French, E.J. Blanz. *J. Med. Chem.*, **9**, 585 (1966).
[19] P. Skehan, R. Storeng, D. Scudiero. *J. Nat. Cancer Inst.*, **82**, 1107 (1990).
[20] W. Geary. *Coord. Chem. Rev.*, **7**, 81 (1981).
[21] M. Akbar Ali, N.E. Hj Ibrahim, R.J. Butcher, J.P. Jasinski, J.M. Jasinski, J.C. Bryan. *Polyhedron*, **17**, 1803 (1998).
[22] D. Boghaei, S. Mohebi. *J. Mol. Catal. A: Chem.*, **179**, 41 (2002).
[23] T.D. Thangadurai, S.K. Ihm. *J. Ind. Eng. Chem.*, **9**, 563 (2003).
[24] T.D. Thangadurai, K. Natarajan. *Transition Met. Chem.*, **26**, 717 (2001).

[25] T. Lobana, G. Bawa, R. Butcher, B. Liaw, C. Liu. *Polyhedron*, **25**, 2897 (2006).
[26] A. El-Sawaf, D. West, F. El-Saied, R. El-Bahnasawy. *Synth. React. Inorg. Met.-Org. Chem.*, **27**, 1127 (1997).
[27] D. Mishra, S. Naskar, M.G.B. Drew, S.K. Chattopadhyay. *Polyhedron*, **24**, 1861 (2005).
[28] S.I. Mostafa, C. Papatriantafyllopoulou, S.P. Perlepes, N. Hadjiliadis. *Bioinorg. Chem. Appl.*, ID 647873 (2008).
[29] K. Nakamoto. *Infrared and Raman Spectra of Inorganic and Coordination Compounds*, 4th Edn, Wiley, New York (1986).
[30] S.I. Mostafa, S. Abd El-Maksoud. *Monatsh Chem.*, **129**, 455 (1998).
[31] W.P. Griffith, S.I. Mostafa. *Polyhedron*, **11**, 2997 (1992).
[32] J. Wiecek, D. Kovala-Demertzi, Z. Ciunik, M. Zervou, M.A. Demertzis. *Bioinorg. Chem. Appl.* (2010). doi:10.1155/2010/867195.
[33] (a) T.S. Lobana, G. Bawa, R.J. Butcher, C.W. Liu. *Z. Anorg. Allg. Chem.*, **635**, 355 (2009); (b) N. Dharmaraj, P. Viswanathamurthi, K. Natarajan. *Transition Met. Chem.*, **26**, 105 (2001).
[34] S.A. Elsayed, A.M. El-Hendawy, I.S. Butler, S.I. Mostafa. *J. Mol. Struct.*, **1036**, 196 (2013).
[35] A.M. Ouf, M.S. Ali, M.S. Soliman, A.M. El-Defrawy, S.I. Mostafa. *J. Korean Chem. Soc.*, **54**, 402 (2010).
[36] S. Halder, S.M. Peng, G.H. Lee, T. Chatterjee, A. Mukherjee, S. Dutta, U. Sanyal, S. Bhattacharya. *New J. Chem.*, **32**, 105 (2008).
[37] (a) I.C. Moreira, P. Juliana, N.L. Speziali, A.S. Mangrich, J.A. Takahashi, H. Beraldo. *J. Braz. Chem. Soc.*, **17**, 1571 (2006); (b) I.C. Mendes, J.P. Moreira, A.S. Mangrich, S.P. Balena, B.L. Rodrigues, H. Beraldo. *Polyhedron*, **26**, 3263 (2007).
[38] M.A. Ali, A.H. Mirza, R.J. Butcher, M.T.H. Tarafder, T.B. Keat, A.M. Ali. *J. Inorg. Biochem.*, **92**, 141 (2002).
[39] F.P.T. Hamers, W.H. Gispen, J.P. Neijt. *Eur. J. Cancer*, **27**, 372 (1991).
[40] H.A. El-Asmy, I.S. Butler, Z.S. Mouhri, B.J. Jean-Claude, M.S. Emmam, S.I. Mostafa. *J. Mol. Struct.*, **1059**, 193 (2014).
[41] J. Zhang, F. Zhang, L. Wang, J. Du, S. Wang, S. Li. *J. Coord. Chem.*, **65**, 2159 (2012).
[42] A.I. Matesanz, P. Souza. *J. Inorg. Biochem.*, **101**, 245 (2007).
[43] (a) S.I. Mostafa. *Transition Met. Chem.*, **24**, 306 (1999); (b) S.I. Mostafa, N. Hadjiliadis. *Transition Met. Chem.*, **33**, 529 (2008).
[44] A.C. Moro, A.C. Urbaczek, E.T. De Almeida, F.R. Pavan, C.Q.F. Leite, A.V.G. Netto, A.E. Mauro. *J. Coord. Chem.*, **65**, 1434 (2012).
[45] V. Cepeda, M.A. Fuertes, J. Castilla, C. Alonso, C. Quevedo, J.M. Perez. *Anti-Cancer Agents Med. Chem.*, **7**, 3 (2007).
[46] I. Kostova. *Recent Patents Anti-Cancer Drug Discov.*, **1**, 1 (2006).

Downloaded by [Institute Of Atmospheric Physics] at 15:20 09 December 2014